arXiv:astro-ph/0602547v1 24 Feb 2006

DISCOVERY OF LYα PUMPED MOLECULAR HYDROGEN EMISSION IN THE PLANETARY NEBULAE NGC 6853 AND NGC 3132

R. E. LUPU, K. FRANCE, AND S. R. MCCANDLISS

Department of Physics and Astronomy, Johns Hopkins University, Baltimore, MD 21218

Draft version February 5, 2008

ABSTRACT

We report the first observation of Lyα pumped molecular hydrogen emission lines in planetary nebulae. The H_2 emission observed in the ultraviolet spectra of NGC 6853 and NGC 3132 can be explained by excitation of vibrationally hot H_2 by Lyα photons. Constraints are placed on the nebular Lyα emission profile, as well as the molecular hydrogen temperature, column density and turbulent motion. These parameters are similar for the two nebulae, pointing to similar physical conditions in these objects. The ro-vibrational cascade following Lyα pumping is predicted to have low surface brightness signatures in the visible and near infrared.

Subject headings: ISM:molecules — planetary nebulae:individual (NGC 6853, NGC 3132) — ultraviolet:ISM

1. INTRODUCTION

Molecular hydrogen emission is often seen in the infrared (IR) observations of photodissociation regions within planetary nebulae (PNe) (Zuckerman & Gatley 1988; Kastner et al. 1996). Continuum pumped ultraviolet (UV) fluorescence, as observed in reflection nebulae and star forming regions (Witt et al. 1989; France & McCandliss 2005), has not been detected in PNe. The observed IR quadrupole emission originates in elevated ro-vibrational levels of the ground electronic state $X^1\Sigma_g^+$. The distribution of molecules in these levels is characteristic of either shock heating (Zuckerman & Gatley 1988) or radiative cascade from excited electronic states (Hayashi et al. 1985; Gatley et al. 1987). UV fluorescence can result in the dissociation of the molecule 10 – 15% of the time (Stecher & Williams 1967), or a non-thermal population in the excited ro-vibrational levels of $X^1\Sigma_g^+$. Shocks, with specific temperatures of $\sim$ 2000 K, can thermally populate higher ro-vibrational states, resulting in IR transitions without the far-UV cascade (Takami et al. 2000). Detection of the UV fluorescence in conjunction with models of the infrared to ultraviolet scaling of H_2 emission can constrain the contribution of each mechanism to the IR flux. The line pumped H_2 UV fluorescence described in this paper is consistent with measured IR line ratios and gas temperatures that favor the shock excitation scenario (Zuckerman & Gatley 1988; Storey 1984). As shown in § 4.1, this type of UV emission, unlike continuum pumped fluorescence, has little effect on the observed IR spectrum. Weak specific features are expected in the optical.

At typical diffuse ISM temperatures below 100 K (Rachford et al. 2002), only H_2 molecules in the v$'' = 0$ level of $X^1\Sigma_g^+$ make a significant contribution to the UV fluorescence. These molecules are excited by $912 \lesssim \lambda \lesssim 1110$ Å radiation into vibrational and rotational levels of higher electronic states (mainly $B^1\Sigma_u^+$ and $C^1\Pi_u$, Black & van Dishoeck 1987). As the temperature increases, higher ro-vibrational levels of $X^1\Sigma_g^+$ become populated, and the threshold for fluorescent pump-

ing moves to progressively larger wavelengths. Due to the long lifetime of the $X^1\Sigma_g^+$ levels, the molecules can be further pumped to $B^1\Sigma_u^+$ or $C^1\Pi_u$ by a sufficiently strong radiation field before they have time to radiate. This mechanism is predicted to be important for nebular gas densities in the range from $10^4 \leq n \leq 10^6$ cm^{-3} and a radiation field (in units of the interstellar average) of $10^3 \leq G_0 \leq 10^4$ (Sternberg 1989).

We have found that in both NGC 6853 (M27, The Dumbbell Nebula) and NGC 3132 H_2 UV fluorescence is dominated by lines pumped by nebular Lyα from the excited v$'' = 2$ level of $X^1\Sigma_g^+$ to the $B^1\Sigma_u^+$ states. Molecular hydrogen resonance fluorescence with Lyα has been previously recognized as an important contributor to the UV flux in collisional environments of photodissociation regions. This effect was first pointed out by Shull (1978), and discussed further by Black & van Dishoeck (1987). Lyα pumping was predicted to be significant mainly for T Tauri stars and Herbig-Haro objects, as has been subsequently observed (Brown et al. 1981; Schwartz 1983; Raymond et al. 1997; Herczeg et al. 2004). Other environments in which Lyα pumping was detected include solar system objects (Wolven et al. 1997; Jordan et al. 1977) and accreting systems (Gizis et al. 2005; Wood et al. 2002). In this paper we present for the first time evidence for resonant excitation by Lyα of the $B - X$ (1 – 2) P(5) 1216.07 Å and $B - X$ (1 – 2) R(6) 1215.73 Å molecular hydrogen lines in planetray nebulae. The observed resonances and line ratios are a valuable diagnostic tool for molecular gas temperature, Lyα line shape, and Doppler shift relative to the H_2 absorber.

The first object, NGC 6853, is a 12,700 year old planetray nebula (O'Dell et al. 2002) at a distance of 417 ± 50 pc (Benedict et al. 2003). Its central star has a temperature $108,600 \pm 6800$ K (Benedict et al. 2003). The distance to NGC 3132 is not well known, varying from 1.63 kpc (Torres-Peimbert & Peimbert 1977) to 0.51 kpc (Pottasch 1996), while the temperature of the ionizing star is estimated at 110,000 K (Pottasch 1996). The extinction, as measured by $E(B - V)$ in this case, is of the order of 0.1 for the central star in

both cases (Benedict et al. 2003; Pottasch 1996). However, McCandliss et al. (2006) argue that in the case of NGC 6853 the extinction is negligible. In both cases, the detected Lyα pumped H$_2$ fluorescence requires a temperature of ~ 2000 K and column densities of $\sim 10^{18}$ cm^{-2}, as well as a Lyα profile of ~ 0.4 Å width, with a deep self-reversal. These parameters satisfy both short and long wavelength constraints, pointing to similar conditions of the molecular gas in the two nebulae.

A description of the observations and data is found in Section 2. Data analysis follows in Section 3, and a discussion of the results in Section 4.

2. OBSERVATIONS

Four nebular observations of NGC 6853 were made by $FUSE$ on 2004 May 26 using the low-resolution (LWRS) aperture ($30'' \times 30''$; Figure 1). Spectra were obtained in the $905 - 1187$ Å bandpass at a filled aperture resolution of ~ 0.33 Å. A description of the $FUSE$ satellite can be found in Moos et al. (2000) and on-orbit performance characteristics are described by Sahnow et al. (2000). The data were acquired as part of the E120 guest observing program. The pointings extend along the bright bar structure of the nebula, from the northeast to the southwest (Figure 1). Data for all four pointings were obtained in "time-tagged" (TTAG) mode, and processed using the CALFUSE pipeline, version 2.4.2. The average exposure time was 3374 seconds. The log of the observations of NGC 6853 is presented in Table 1.

We obtained optical spectra of NGC 6853 on 1999 June 9 using the Double Imaging Spectrograph (DIS) on the Apache Point 3.5m telescope. The observations were taken with the low-resolution gratings, centered at 8000 Å and 4224 Å with a dispersion of 7.0 Å pixel^{-1} in the red side and 6.1 Å pixel^{-1} in the blue side, and a resolution of roughly 2 pixels. The $300'' \times 0''.9$ slit was centered at (19^h 59^m $36^s.20$, $22°$ $43'$ $01''.00$), and oriented along the bright bar. Three slit positions (about $2''.7$ total width) were averaged during the 900 s integration. The observed mean Hα brightness along the slit was about 4.68×10^{-3} ergs cm^{-2} s^{-1} sr^{-1}, or 19416 R (conversion factor 632 $\lambda_{H\alpha}$(Å)).

NGC 3132 was observed by HUT aboard $Astro - 2$ for 946 seconds during orbital night on 1995 March 14. This spectrum, downloaded from the Multi-Mission Archive at the Space Telescope Science Institute (MAST), was acquired through the $10'' \times 56''$ slit, enclosing a large region of the $28''$ nebula, at an offset from the central stars. The exact slit coordinates are uncertain. The resolution of the HUT spectrum is roughly 3 Å. A description of the HUT instrument and data reduction can be found in Kruk et al. (1995). The signature of H$_2$ emission is present in the $FUSE$ spectrum of NGC 3132 (D1200401), but at a considerably lower signal-to-noise ratio. We chose to analyze the HUT spectrum because it allowes us to extend our study to longer wavelengths.

3. DATA ANALYSIS

3.1. *NGC 6853*

The $FUSE$ spectra of NGC 6853 – Position 3 are presented in Figure 2 and Figure 3. The emission from the nebula is dominated by He II, C II, C III and molecular hydrogen lines. The strongest lines observed in all four pointings are summarized in Tables 2-5. The lines
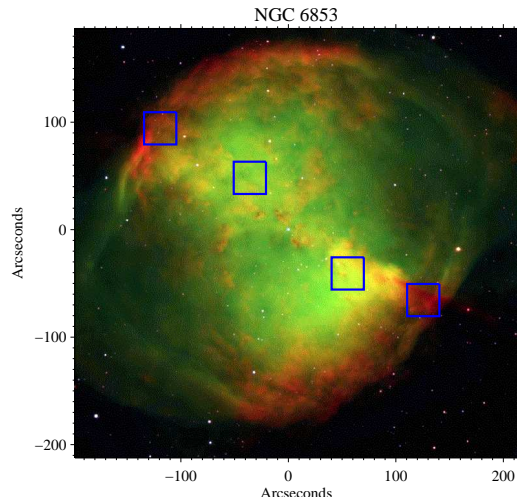

FIG. 1.— Optical image of NGC 6853 obtained during the commissioning of the FORS1 instrument on the VLT 8.2-m. This three color image was made from a composite of B, [O III], and Hα filters. $FUSE$ LWRS aperture overlays are imposed showing the location of the four nebular pointings 1 to 4 from left to right. The optical image was obtained from the European Southern Observataory.

denoted by letters $A - D$ are unidentified. Feature A is possibly nebular O III (962.425 Å) at a slight velocity offset. The strengths of the lines in the spectrum changes with the pointing. The highly ionized species dominate in the central regions and decline towards the outer shell. Molecular hydrogen lines are present in all four pointings, and are strongest in the third pointing, which coincides with the brightest optical feature.

We explored the possibility that line-pumped H$_2$ fluorescence is responsible for some of the unidentified lines we observe, computing models with a variety of nebular emission lines as the excitation source. Atomic emission lines of H I Ly-β, Ly-δ, and Ly-γ; He II $\lambda1215$, $\lambda1085$, $\lambda1025$, $\lambda992$, and $\lambda959$; C II $\lambda\lambda1334/35$ and $\lambda\lambda1036/37$; the C III $\lambda1175$ multiplet and C III $\lambda977$; N I $\lambda1200$; the N II $\lambda1085$ multiplet; the N III $\lambda990$ multiplet; and the O VI resonance doublet $\lambda\lambda1032/38$ were all considered as possible H$_2$ excitation mechanisms. None of the strongest predicted fluorescent emission lines are observed.

The strongest H$_2$ lines observed are excited by the $B - X$ $(1 - 2)$ P(5) transition at 1216.07 Å in the red wing of Lyα. Their wavelengths and branching ratios are listed in Table 6. These transitions are sensitive to the Lyα line width and Doppler shift. Although the closest resonance is $B - X$ $(1 - 2)$ R(6) at 1215.73 Å, Lyman-system fluorescence from v' = 1, J' = 7 is far weaker than expected. This can be achieved with a deep self-reversal of the Lyα profile combined with a blueshifting of the molecular hydrogen lines with respect to the systemic Lyα emission. The bueshift is necessary to restore to some extent the intensities of the lines pumped by the $(1 - 2)$ R(6) resonance, which otherwise would fall in the center of the absorption trough (Figure 4).

NGC 6853, as well as NGC 3132, was modeled using

TABLE 1
FUSE OBSERVATIONS OF NGC 6853.

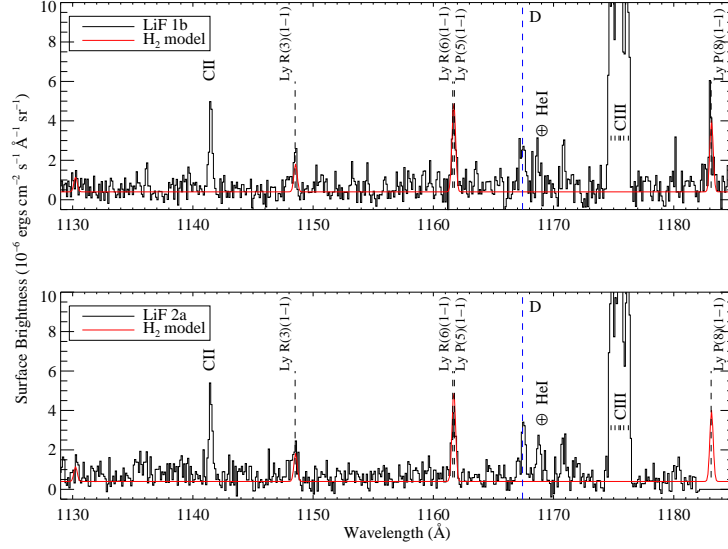| Instrument	Program	Date	RA	Dec	Exp. Time (s)
FUSE - LWRS	E12001	2004-05-26	19 59 44.96	+22 44 50.1	4176.0
FUSE - LWRS	E12002	2004-05-26	19 59 38.93	+22 44 04.0	3071.0
FUSE - LWRS	E12003	2004-05-26	19 59 32.35	+22 42 35.1	2778.0
FUSE - LWRS	E12004	2004-05-26	19 59 27.27	+22 42 10.3	3470.0

FIG. 2.— *FUSE* spectra of NGC 6853 at the third pointing. Both the LiF 1b (upper) and LiF 2a (lower) channels are shown to cover the whole 1115 – 1187 Å interval. The H₂ emission is prominent together with C II, C III and geocoronal He I. The Lyα pumped H₂ fluorescence model is shown in red.
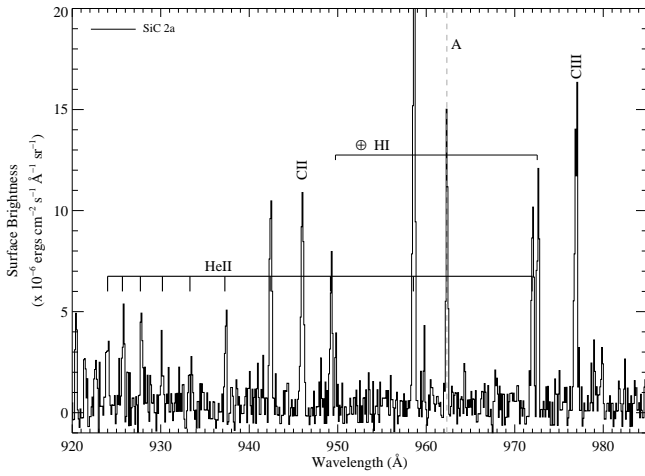

FIG. 3.— The short wavelength FUSE SiC 2a spectrum of NGC 6853 at the third pointing. Strongest features are nebular He II, C II, C III and geocoronal H I.
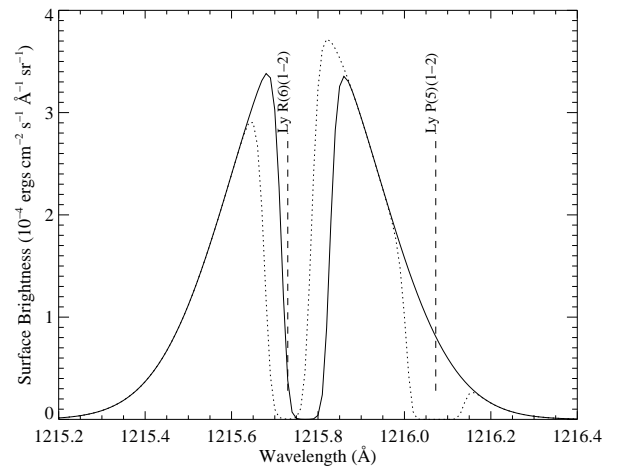

FIG. 4.— Exciting Lyα profile absorbed by a H I column density of 1×10^{14} cm^{-2} used for the NGC 6853 model. Velocity offsets with respect to the molecular hydrogen reference system are 25 km s^{-1} for both emission and H I absorption. The H₂ absorbing transitions are indicated by dashed lines. The dotted line corresponds to an H₂ absorption profile for a column density of 6×10^{18} cm^{-2}.

a fluorescent H₂ emission code similar to the one de-

TABLE 2
NGC 6853 Position 1.

Line ID	λ_{obs} (Å)	FWHM (Å)	Brightness (10^{-6} ergs cm^{-2} s^{-1} sr^{-1})
C II	946.01	0.56	1.83 ± 0.29
He II	958.52	0.53	0.35 ± 0.28
N III + He II	991.52	0.21	1.91 ± 0.39
C II	1036.88	0.33	1.37 ± 0.22
N II + He II	1085.50	0.34	25.75 ± 1.03
C II	1141.53	0.26	0.36 ± 0.13
H$_2$(1–1)R(3)	1148.59	0.43	0.40 ± 0.14
H$_2$(1–1)P(5) + R(6)	1161.76	0.32	0.71 ± 0.16
C III	1175.53	0.48	1.97 ± 0.23
H$_2$(1–1)P(8)	1183.06	0.21	0.92 ± 0.32

NOTE. — The C III line at 977.03 Å is not listed due to contamination from scattered solar light in the SiC channels.

TABLE 3
NGC 6853 Position 2.

Line ID	λ_{obs} (Å)	FWHM (Å)	Brightness (10^{-6} ergs cm^{-2} s^{-1} sr^{-1})
He II	933.35	0.26	1.57 ± 0.43
He II	937.24	0.21	0.78 ± 0.37
He II	942.43	0.29	6.15 ± 0.50
C II	946.02	0.46	5.16 ± 0.48
He II	949.24	0.43	2.83 ± 0.38
He II	958.59	0.29	12.37 ± 0.61
Un-ID (A)	962.31	0.27	4.24 ± 0.48
N III + He II	992.30	0.31	48.83 ± 1.28
S III	1015.48	0.89	1.65 ± 1.08
S III	1021.32	0.68	0.72 ± 0.25
C II	1036.90	0.42	3.59 ± 0.34
Un-ID (B)	1062.62	0.44	0.31 ± 0.28
Un-ID (C)	1065.84	0.47	0.98 ± 0.27
N II + He II	1084.79	0.32	130.94 ± 2.46
C II	1141.51	0.37	1.26 ± 0.23
H$_2$(1–1)R(3)	1148.63	0.23	0.62 ± 0.23
H$_2$(1–1)P(5) + R(6)	1161.75	0.40	1.62 ± 0.23
Un-ID (D)	1167.30	0.51	1.24 ± 0.27
C III	1175.53	1.02	45.55 ± 0.78
H$_2$(1–1)P(8)	1183.26	0.35	2.01 ± 0.51

TABLE 4
NGC 6853 Position 3.

Line ID	λ_{obs} (Å)	FWHM (Å)	Brightness (10^{-6} ergs cm^{-2} s^{-1} sr^{-1})
He II	933.40	0.54	1.21 ± 0.36
He II	937.30	0.26	0.91 ± 0.34
He II	942.46	0.30	3.63 ± 0.44
C II	946.03	0.39	4.75 ± 0.44
He II	949.30	0.22	2.06 ± 0.33
He II	958.63	0.29	8.86 ± 0.54
Un-ID (A)	962.35	0.27	3.69 ± 0.45
N III + He II	992.34	0.32	30.27 ± 1.02
S III	1015.42	0.81	1.20 ± 0.32
S III	1021.16	0.52	0.57 ± 0.20
C II	1036.81	0.33	2.37 ± 0.29
Un-ID (B)	1062.34	0.31	0.20 ± 0.25
Un-ID (C)	1065.79	0.30	1.40 ± 0.26
N II + He II	1084.82	0.34	95.18 ± 2.18
C II	1141.48	0.31	1.50 ± 0.22
H$_2$(1–1)R(3)	1148.48	0.42	0.68 ± 0.23
H$_2$(1–1)P(5) + R(6)	1161.70	0.42	1.33 ± 0.22
Un-ID (D)	1167.44	0.50	1.65 ± 0.26
C III	1175.48	1.07	28.33 ± 0.65
H$_2$(1–1)P(8)	1183.05	0.26	3.17 ± 0.49

TABLE 5
NGC 6853 Position 4.

Line ID	λ_{obs} (Å)	FWHM (Å)	Brightness (10^{-6} ergs cm^{-2} s^{-1} sr^{-1})
C II	946.05	0.38	1.22 ± 0.30
He II	958.59	0.24	0.34 ± 0.32
N III + He II	991.63	0.32	1.56 ± 0.42
C II	1037.75	0.42	0.56 ± 0.22
N II + He II	1085.54	0.34	18.76 ± 0.97
C II	1141.52	0.25	0.21 ± 0.14
H$_2$(1–1)R(3)	1148.50	0.27	0.12 ± 0.14
H$_2$(1–1)P(5) + R(6)	1161.73	0.21	0.66 ± 0.17
C III	1175.56	0.29	1.29 ± 0.23
H$_2$(1–1)P(8)	1183.18	0.31	1.49 ± 0.34

scribed in France et al. (2005). The exciting radiation field was assumed to be a Gaussian Lyα emission line, with a FWHM of 0.4 Å. In order to mimic self-reversal, absorption by neutral hydrogen with a column density of 1×10^{14} cm^{-2} was used to modify the exciting Lyα profile (Figure 4). As the nebular Lyα line cannot be measured directly due to the opacity of the ISM and contamination from geocoroanal Lyα, a total brightness was chosen as 2/3 of the Hα brightness of 19416.0 R measured using the DIS at APO (see § 2). According to the selection rules, 2/3 of the time the Hα transitions will result in an atom in the $2p$ state, which can then radiate a Lyα photon during the $2p - 1s$ transition. The other 1/3 of the time, the hydrogen atom will be left in the $2s$ state, unable to emit a Lyα photon since a direct transition from this state to $1s$ is forbidden in the dipole approximation (Spitzer 1978). The total Lyα brightness could be higher than derived from Hα measurements, due to H$_2$ dissociation mechanisms that produce H I in the $2p$ state (Glass-Maujean 1986). The continuum flux

from the central star of NGC 6853 has not been included because continuum pumped emission lines are not detected in the nebular spectra. The likely explanation for the absence of continuum pumped fluorescence resides in the dominance of Lyα photons over the 912 – 1110 Å stellar continuum as well as the small covering factor involved in the absorption of continuum radiation, as will be discussed in § 4.

The model parameters summarized in Table 7 were adjusted to reproduce the 1115 – 1187 Å line strengths observed in the LiF 1B channel. The LiF 2A channel (Figure 2) shows a 20% decrease in the (1–1) R(3) brightness, which we attribute to calibration offsets. The molecular hydrogen temperature of 2040 K was derived from absorption spectra (McCandliss et al. 2006). The H$_2$ absorption is blueshifted with respect to the Lyα profile by about –25 km s^{-1}, value supported by recent studies of NGC 6853 (McCandliss et al. 2006), assuming Lyα at the systemic velocity. The choosen total Lyα brightness constrains the molecular hydrogen column density of 6×10^{18} cm^{-2}. An H$_2$ column density of few $\times 10^{16}$ cm^{-2}, as inferred from absorption spectra

TABLE 6
Lyman system transitions pumped by Lyα out of the
(v″,J″) levels (2,5) and (2,6).

Line ID	Wavelength (Å)	Branching Ratio ($\times 10^4$)
(1– 0) R(3)	1096.73	76.6116
(1– 0) P(5)	1109.31	100.7527
(1– 1) R(3)	1148.70	389.9806
(1– 1) P(5)	1161.82	492.7111
(1– 2) R(3)	1202.45	778.3324
(1– 2) P(5)	1216.07	926.0875
(1– 3) R(3)	1257.83	693.4022
(1– 3) P(5)	1271.93	742.2661
(1– 4) R(3)	1314.62	168.5805
(1– 4) P(5)	1329.14	124.0794
(1– 5) R(3)	1372.49	48.7069
(1– 5) P(5)	1387.37	123.9049
(1– 6) R(3)	1431.01	580.3754
(1– 6) P(5)	1446.12	825.4512
(1– 7) R(3)	1489.57	944.7024
(1– 7) P(5)	1504.76	1149.4655
(1– 8) R(3)	1547.34	667.8068
(1– 8) P(5)	1562.39	713.7622
(1– 9) R(3)	1603.25	217.7934
(1– 9) P(5)	1617.89	196.6773
(1–10) R(3)	1655.93	23.3209
(1–10) P(5)	1669.77	14.8395
(1–11) R(3)	1703.59	0.0253
(1–11) P(5)	1716.13	0.0397
(1–12) R(3)	1744.02	0.0834
(1–12) P(5)	1754.61	0.0423
(1–13) R(3)	1774.47	0.0090
(1–13) P(5)	1782.18	0.0110
(1–14) R(3)	1791.53	0.0006
(1– 0) R(6)	1109.86	69.9280
(1– 0) P(8)	1130.40	88.4209
(1– 1) R(6)	1161.95	377.8252
(1– 1) P(8)	1183.31	447.6342
(1– 2) R(6)	1215.73	809.8802
(1– 2) P(8)	1237.87	873.5052
(1– 3) R(6)	1271.02	797.9877
(1– 3) P(8)	1293.87	729.6058
(1– 4) R(6)	1327.56	247.0670
(1– 4) P(8)	1351.04	133.2556
(1– 5) R(6)	1385.01	22.8098
(1– 5) P(8)	1408.96	111.5518
(1– 6) R(6)	1442.87	554.2507
(1– 6) P(8)	1467.08	800.3663
(1– 7) R(6)	1500.45	1009.0800
(1– 7) P(8)	1524.65	1111.9502
(1– 8) R(6)	1556.87	743.2822
(1– 8) P(8)	1580.67	653.4937
(1– 9) R(6)	1610.95	236.9584
(1– 9) P(8)	1633.84	152.5215
(1–10) R(6)	1661.20	20.8714
(1–10) P(8)	1682.49	6.1068
(1–11) R(6)	1705.68	0.0395
(1–11) P(8)	1724.43	0.3495
(1–12) R(6)	1741.95	0.0684
(1–12) P(8)	1756.90	0.0004
(1–13) R(6)	1766.87	0.0179

(McCandliss et al. 2006) would require a much higher Lyα brightness.

3.2. *NGC 3132*

In analyzing the NGC 3132 spectrum it is important to account for the background. The continuum has a very unusual shape, most likely due to the superposition of the central stars and the inhomogeneous dust distribution within the nebula. A detailed analysis of the continuum is beyond the scope of this work, but a

TABLE 7
H₂ Model Parameters.

Parameter	NGC 6853	NGC 3132
Excitation Source	H I Lyα	H I Lyα
Lyα Doppler shift	25 km s^{-1}	30 km s^{-1}
Lyα FWHM	0.40 Å	0.45 Å
Lyα total intensity	12944 R	217523 R
T(H₂)	2040 K	2040 K
N(H₂)	6.0×10^{18} cm^{-2}	3.0×10^{18} cm^{-2}
N(H I)	1.0×10^{14} cm^{-2}	2.0×10^{16} cm^{-2}
b	8 km s^{-1}	9 km s^{-1}

TABLE 8
NGC 3132.

Line ID	λ_{obs} (Å)	FWHM (Å)	Brightness (10^{-6} ergs cm^{-2} s^{-1} sr^{-1})
H₂(1–3)R(3)	1259.19	4.14	8.62 ± 0.48
H₂(1–3)P(5)	1273.38	3.57	16.81 ± 0.52
H₂(1–6)R(3)	1431.73	2.41	11.86 ± 0.53
H₂(1–6)P(5)	1446.67	4.01	26.75 ± 0.62
H₂(1–7)R(3)	1489.85	2.27	23.12 ± 0.64
H₂(1–7)P(5)	1505.84	2.41	22.59 ± 0.58
H₂(1–8)R(3)	1548.16	2.89	15.54 ± 0.64
H₂(1–8)P(5)	1563.10	1.92	14.35 ± 0.64
H₂(1–9)P(5)	1617.69	1.28	7.04 ± 0.75

rough baseline is needed for the model H₂ spectrum. We set this background by manipulating the original HUT spectrum to extract a smooth continuum curve. A broad (width ∼ 75 Å) median filter was applied to the data at wavelengths between 1100 and 1750 Å to remove most of the nebular and geocoronal emission lines. A boxcar smooth (width ∼ 20 Å) was then applied, leaving a background continuum spectrum. Measured brightnesses for the strongest lines are given in Table 8. The observed H₂ emission lines provide a long wavelength confirmation of pumping by Lyα photons.

We use the NGC 6853 model as a starting point for NGC 3132 as a detailed study of the molecular structure of NGC 3132 was not available. Previous observations and models of NGC 3132 (Monteiro et al. 2000; Bässgen et al. 1990) estimate the nebular Hα luminosity at ∼ few × 10^{44} photons s^{-1}, too low to predict the observed level of H₂ fluorescence. This value was derived using a distance of 670 pc, which might be an underestimate. The estimated total Hα luminosity of NGC 6853, approximated as an elliptical nebula with semimajor axes of 2′.5 and 4′, at a distance of 417 pc, is 8.55 × 10^{46} photons s^{-1}. Using for the NGC 3132 0′.45×0′.7 nebula a total Hα luminosity of ∼ 1 × 10^{47} photons s^{-1}, closer to the value for NGC 6853, we obtain a reasonable fit with column densities of 3 × 10^{18} cm^{-2} for the molecular component and 2 × 10^{16} cm^{-2} for the atomic hydrogen. The molecular hydrogen absorption is blueshifted with respect to the nebular Lyα by –30 km s^{-1}, in agreement with other measurements (Monteiro et al. 2000). A summary of the parameters used is given in Table 7. The overprediction of line strengths in the 1200 ≤ λ ≤ 1300 Å region (Figure 5)
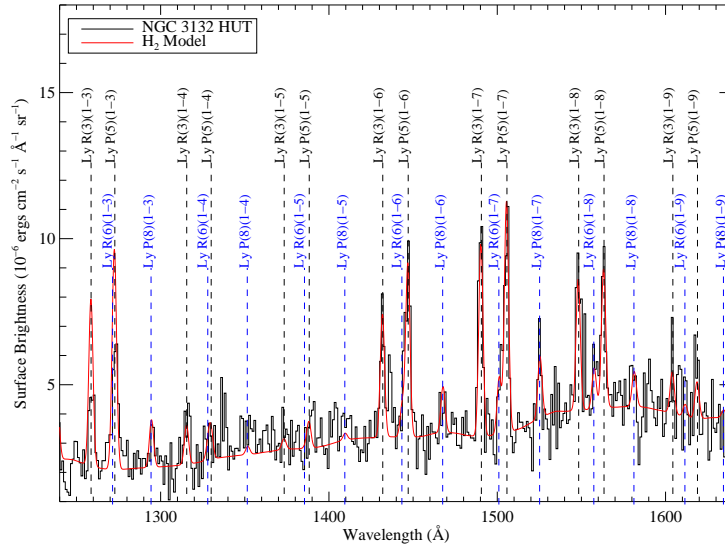
Fig. 5.— HUT spectrum of NGC 3132. The H$_2$ model added to an empirical fit to the continuum is shown in red (see text).

and shortward of 1200 Å (not shown) is caused by an incomplete removal of the combination of geocoronal Lyα and the $(1-3)$ H$_2$ emission band together with opacity effects. These shorter wavelength lines connect to more populated lower vibrational levels (Table 6), leading to self-absorption (Herczeg et al. 2004; Wood et al. 2002).

4. DISCUSSION

Although H$_2$ absorption was observed in both nebulae (McCandliss et al. 2006; Sterling et al. 2002), continuum pumped molecular hydrogen emission was not detected. Predicted continuum pumped UV fluorescence for an H$_2$ column density of 7.9×10^{16} cm^{-2}, measured from absorption spectra (McCandliss et al. 2006), is estimated at a level of $\sim 0.7 \times 10^{-6}$ ergs cm^{-2} s^{-1} sr^{-1} Å^{-1}, consistent with the noise level in Figure 2. However, the larger column density used in the Lyα pumping model, would predict a much higher continuum fluorescence, which is not observed. One possible explanation comes from the dominance of Lyman continuum photons over the $912-1110$ Å photons which contribute to continuum H$_2$ pumping. In the central H II region of a PN, Lyman continuum photons are readily converted into Lyα line photons, following a series of ionizations, recombinations and cascades. Integrating a stellar model with T$_{eff}$ = 110,000 K, $\log(g)$ = 6.7, and M$_\star$ = 0.56 M$_\odot$ (Rauch 2003), we find that there are over 16 times more photons cm^{-2} s^{-1} emitted in the Lyman continuum $(5-911.7$ Å) than in the $912-1110$ Å region. Additionally, the Lyman continuum photons are concentrated into an emission line (FWHM$_{Ly\alpha}$ = 0.4 Å), compared with the far-UV stellar continuum that spans roughly 200 Å. For an H II region with an electron temperature of 12,000 K (i.e.- NGC 6853; Pottasch et al. (1982)) the recombination efficiency for generating Lyα photons is roughly 67% (Spitzer 1978), which gives us 5.5×10^{45} photons s^{-1}. The total Lyα luminosity obtained this way is still low

compared to the value of 8.55×10^{46} photons s^{-1} derived from the Hα brightness. This shows that the ratio of Lyα photons to $912-1110$ Å continuum photons might be even higher than estimated.

However, the dominance of Lyα photons over the $912-1110$ Å stellar continuum alone is not sufficient to compensate for the larger ground state populations and higher oscillator strengths contributing to other Lyman and Werner transitions out of v$''$ = 0. Assuming that molecules reside in high density globules, the covering factor involved in continuum excitation is much smaller than for the diffuse radiation field of scattered Lyα. If we let B$_0$ be the surface brightness of the exciting field, the total flux absorbed by an H$_2$ clump will be B$_0\Omega$, where Ω is the solid angle subtended by the absorber, as seen from the source. The redistributed brightness is then radiated into 4π, so that we can define an effective surface brightness seen by the absorber as (B$_0\Omega$) / 4π, where Ω / 4π is the covering factor. For a $10'' \times 10''$ globule at a $50''$ separation from the central star, the continuum covering factor is about 0.0032, while for the nebular Lyα it is likely to be unity. This estimate takes into account that, while the continuum photons are coming mainly from the star, the Lyα photons are produced and scattered in the nebula, so that the globules are effectively embedded in a diffuse Lyα radiation field covering all 4π sr.

The broad (98.6 km s^{-1} FWHM) Lyα line required to pump the H$_2$ lines in NGC 6853 is likely to originate in the complex shell structure of the nebula. As shown by Meaburn et al. (2005), in the case of Hα the wide profile is a result of combining the motions of the outer shell at 35 km s^{-1}, the inner shell at 13 km s^{-1} and the bulk motion less than 7 km s^{-1} in the central He II region. We infer a similarly broad velocity structure should be present in NGC 3132 to produce a Lyα of comparable width. A narrower velocity distribution would be allowed if we take into account the redistribution of the

Lyα photons in the line wings for large optical depths.

IR observations of NGC 6853 and NGC 3132 made to date (Storey 1984; Zuckerman & Gatley 1988) conclude that the H₂ spectrum is shock excited based on the ratios of the S(1) (1–0) and S(1) (2–1) lines. Moreover, this conclusion is supported by the non-detection of continuum pumped UV fluorescence, both in these spectra and in rocket observations of the Dumbbell (McCandliss 2001). However, recent studies (Hora et al. 1999; Takami et al. 2000) show that in dense enough environments the ratio of the S(1) (1–0) and S(1) (2–1) lines can appear thermal, even if the IR emission is excited via UV pumping. In these cases, the study of transitions from higher energy levels becomes important in order to distinguish between the two mechanisms. The detection of H₂ continuum absorption towards the central star of NGC 6853 shows that continuum pumped fluorescence takes place, although at a level allowed by a non-detection in the *FUSE* spectra. This by itself does not rule out a partial UV continuum pumping of the IR lines. However, the thermal processes are thought to be dominant, since absorption out of vibrational levels v″ > 2 is not observed, in contrast with reflection nebulae where fourescence is important (Meyer et al. 2001). The possibility of shock excitation in NGC 6853 and NGC 3132 is also revealed here by the high temperature required by the presence of Lyα pumping. More in-depth analysis of PNe (Hora et al. 1999; Davis et al. 2003) reveal that in most cases where both the rotational and vibrational temperature of H₂ are around 2000 K, shock heating is the dominant excitation mechanism of IR lines. In order to confirm the shock scenario, we need a better understanding of the gas motions in the two objects, in addition to observations shortward of 2 μm.

The observed presence of both ionized species and molecules in the same aperture, and the small covering factor necessary to explain the non-detection of continuum pumped lines confirms the current view of molecules residing in globules surrounded by an ionized medium, the source of the exciting Lyα radiation (Meaburn & Lopez 1993; Huggins et al. 2002; Speck et al. 2003). The presence of globules helps the survival of hydrogen molecules, shielded from photodissociation by hard stellar radiation. Overall, the H₂ column density derived for the Ly alpha pumping model is much higher than the one derived from absorption spectra (10^{18} cm^{-2} vs 10^{16} cm^{-2}), suggesting different properties of the regions they are probing. Taking into account that the globule size in NGC 6853 is likely to be less than 10", the *FUSE* observations average between high and low density areas, where the low density regions are thought to have a negligible extinction. The low slit filling fraction for the Lyα pumped radiation in both *FUSE* and *HUT* observations allows us to reconcile the derived value of few×10^{18} cm^{-2} for the H₂ column density with coulmns of 10^{21} cm^{-2} suggested for dense globules from visual exctinction arguments (Bohlin et al. 1978; Meaburn & Lopez 1993).

4.1. *Ro-vibrational Cascade Modified by Lyα Pumping*

We constructed the ro-vibrational spectrum as a combination of a non-equilibrium cascade following Lyα pumping and a steady state emission due to the equilibrium distribution of molecules on the $X^1\Sigma_g^+$ state levels.

For the non-equilibrium cascade, we start with the rates at which the $X^1\Sigma_g^+$ levels are populated following Lyα pumping, and evaluate the line strengths according to the branching ratios. Collisional effects are ignored for the purpose of this estimate. As a proxy for the equilibrium populations for the steady state case we use the ground state populations measured from absorption spectra and extrapolated to higher vibrational and rotational levels using a 2040 K thermal distribution with a total H₂ column density of 7.9×10^{16} cm^{-2}. For this reason hereafter we will refer to this steady state model as thermal. The transition probabilities from Wolniewicz et al. (1998) are used to derive the output spectrum, shown in Figure 6. The solid black line contains contributions from both thermal and fluorescent pumping, convolved with a 15 Å Gaussian. Overplotted in red is the thermal contribution alone. The lines showing the largest contribution from fluorescent pumping are numbered, and their principal components are listed in Table 9. The line strengths are given as upper limits and will be affected by collisional de-excitation. Collisional excitation is not important for these high lying vibrational states. Using for the thermal model the same total H₂ column density of 6×10^{18} cm^{-2} used for the Lyα pumping, the lines with the highest contribution from fluorescent cascade will be 1,2,3,4,8,9 and 10, as numbered in Figure 6.

The ro-vibrational cascade shows most of the Lyα pumping specific features in the visible and near-IR part of the spectrum. We find little deviation from a pure thermal emission longward of ∼ 1 μm. As a consequence, line pumped UV fluorescence might be present even when the measured IR line ratios around 2 μm are consistent with a thermal distribution of the H₂ molecules in the ground electronic state.

The detection of these lines represents an observational challenge from the ground. In Figure 8 the positions of the strongest predicted lines are indicated on the airglow emission spectrum reconstructed from UVES observations (Hanuschik 2003) at a resolution of 15 Å to match the resolution of our model. The lack of airglow features in the 0.577 – 0.583 μm interval is due to the chip gap in the UVES spectrum. However, Osterbrock et al. (1996) shows that there are no lines identified in this region. The ro-vibrational cascade at a level of few × 10^{-5} ergs cm^{-2} s^{-1} sr^{-1} μm^{-1} is about 1000 times smaller than the typical airglow lines and contiuum in the 0.56 – 1.015 μm interval. A much lower background level and a higher spectral resolution (∼ few Å) may allow the detection of the (9–3) S(4) line at 5810.36 Å and the (8–3) S(6) line at 6681.40 Å (Figure 7).

Lyα pumping redistributes molecules from the (v″,J″) levels (2,6) and (2,5) among the ro-vibrational levels of the ground state. However, at the level of the observed UV fluorescence, a significant deviation from the thermal populations of the (v″,J″) levels (2,6) and (2,5) is not found. Correcting for the ro-vibrational transitions that repopulate these levels, we find that the population decrease relative to the thermal distribution (Δ N$_{vJ}$/N$_{vJ}^{thermal}$) is about 0.0107 and 0.0012 for the (2,6) and (2,5) levels respectively. We find more significant deviations from a thermal population among the rotational levels of the v″=0 state. These are likely to be af-
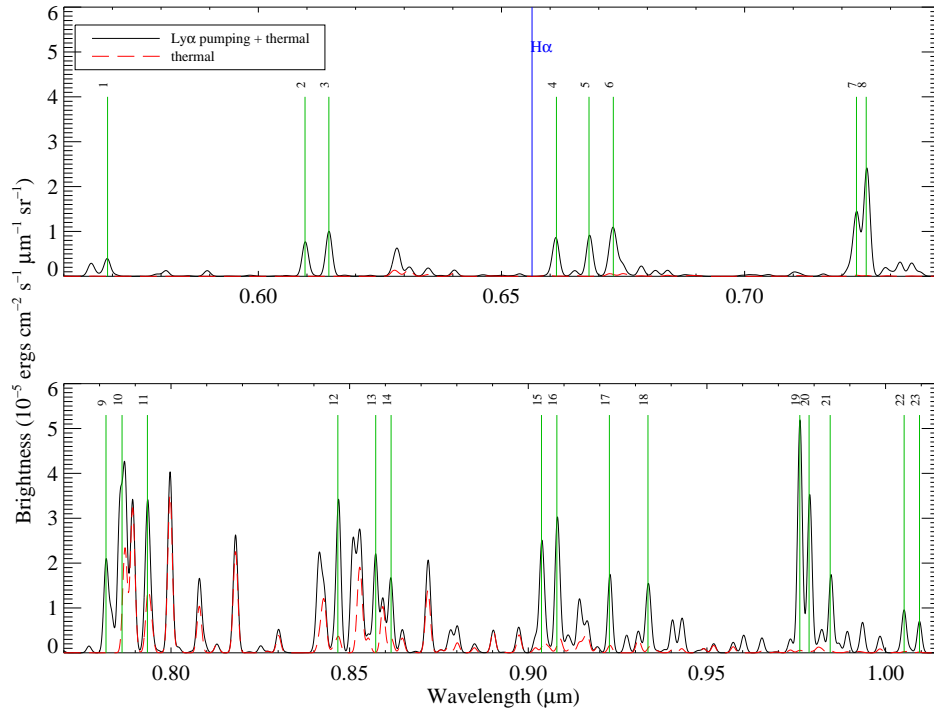
FIG. 6.— Predicted ro-vibrational cascade following Lyα pumping in NGC 6853 (see text). The red dashed line is the ro-vibrational cascade model for a thermal population at 2040 K. The black continuous line has both contributions added. The main contributors to the numbered lines are listed in Table 9.
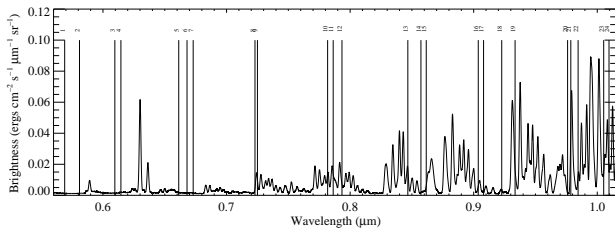

FIG. 7.— Airglow spectrum reconstructed from UVES data (Hanuschik 2003), with a resolution of 15 Å. The positions of the strongest lines following Lyα pumping are indicated by the green lines, numbered as in Figure 6.

NGC 6853 and NCG 3132. The observed H_2 fluorescence gives us valuable information about the conditions of the radiation field and dynamics of the molecular gas in planetary nebulae. The input parameters are similar for both objects, suggesting that we do not see an isolated phenomenon. The UV H_2 spectrum is likely due to thermally excited molecular hydrogen, shielded from the UV continuum inside globules surrounded by strong nebular Lyα emission. We emphasize that while molecular hydrogen pumping by Lyα shows strong features in UV spectra, it could remain unobservable in the IR and visible. UV observations are thus a requirement for investigating this process in various environments where hot H_2 is exposed to the presence of Lyα.

fected also by collisional redistribution and do not match the deviations measured from UV absorption spectra (McCandliss et al. 2006). Deviations in the populations of higher vibrational levels ($v'' > 2$) are predicted to result in a specific signature in the ro-vibrational spectrum (Figure 6).

5. CONCLUSION

Line pumping by Lyα is required to qualitatively explain the H_2 emission features in the far UV spectra of

REFERENCES

Bässgen, M., Diesch, C., & Grewing, M. 1990, A&A, 237, 201
Benedict, G. F., et al. 2003, AJ, 126, 2549

Black, J. H., & van Dishoeck, E. F. 1987, ApJ, 322, 412
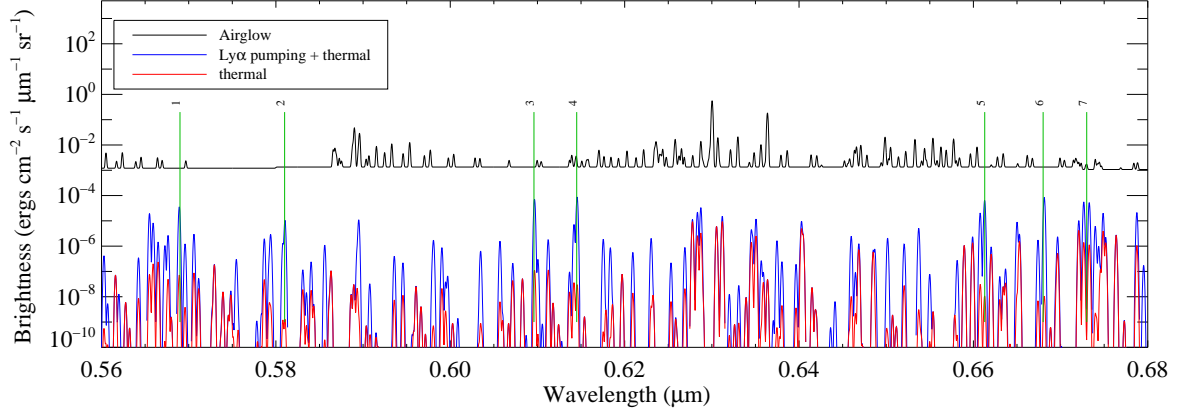Bohlin, R. C., Savage, B. D., & Drake, J. F. 1978, ApJ, 224, 132

FIG. 8.— Airglow spectrum and ro-vibrational cascade at a resolution of 1.6 Å, on a logarithmic scale. The black line is the airglow spectrum, while the red and blue are the thermal and co-added (thermal + fluorescent) models, respectively.

TABLE 9
Ro-vibrational cascade, thermal contribution not included.

Ref No	Line ID	Wavelength (Å)	Brightness (R)
1	(6–1) S(6)	5689.17	0.022
2	(9–3) S(4)	5810.36	0.007
3	(7–2) S(4)	6096.58	0.034
3	(7–2) S(3)	6096.74	0.013
4	(7–2) S(6)	6145.49	0.058
5	(8–3) S(3)	6607.73	0.015
5	(8–3) S(4)	6612.89	0.047
6	(8–3) S(6)	6681.40	0.061
7	(5–1) S(4)	6726.46	0.040
7	(5–1) S(6)	6732.89	0.037
8	(9–4) S(4)	7224.75	0.024
8	(6–2) S(4)	7231.36	0.082
9	(6–2) S(3)	7250.86	0.036
9	(6–2) S(6)	7251.65	0.134
10	(7–3) S(4)	7818.21	0.160
10	(7–3) S(3)	7833.48	0.064
11	(7–3) S(6)	7857.03	0.240
11	(3–0) S(6)	7871.01	0.120
12	(3–0) S(4)	7934.81	0.150
13	(4–1) S(4)	8469.30	0.255
14	(8–4) S(6)	8572.68	0.189
15	(4–1) S(2)	8615.89	0.093
16	(5–2) S(6)	9037.36	0.203
17	(5–2) S(4)	9081.00	0.252
18	(4–1) Q(4)	9228.52	0.034
18	(5–2) S(2)	9228.82	0.113
19	(9–5) S(4)	9333.02	0.069
19	(9–5) S(3)	9333.40	0.021
19	(5–2) S(1)	9339.80	0.065
20	(6–3) S(5)	9758.45	0.019
20	(6–3) S(6)	9760.54	0.486
21	(6–3) S(4)	9787.93	0.345
22	(6–3) S(3)	9847.38	0.170
23	(6–3) S(1)	10052.00	0.092
24	(5–2) Q(6)	10095.00	0.070

Brown, A., Jordan, C., Millar, T. J., Gondhalekar, P., & Wilson, R. 1981, Nature, 290, 34

Davis, C. J., Smith, M. D., Stern, L., Kerr, T. H., & Chiar, J. E. 2003, MNRAS, 344, 262

France, K., Andersson, B.-G., McCandliss, S. R., & Feldman, P. D. 2005, ApJ, 628, 1

France, K., & McCandliss, S. R. 2005, ApJ, 629, L97

Gatley, I., et al. 1987, ApJ, 318, L73

Gizis, J. E., Shipman, H. L., & Harvin, J. A. 2005, ApJ, 630, L89

Glass-Maujean, M. 1986, Phys. Rev. A, 33, 342

Hanuschik, R. W. 2003, A&A, 407, 1157

Hayashi, M., Hasegawa, T., Gatley, I., Garden, R., & Kaifu, N. 1985, MNRAS, 215, 31P

Herczeg, G. J., Wood, B. E., Linsky, J. L., Valenti, J. A., & Johns-Krull, C. M. 2004, ApJ, 607, 369

Hora, J. L., Latter, W. B., & Deutsch, L. K. 1999, ApJS, 124, 195

Huggins, P. J., Forveille, T., Bachiller, R., Cox, P., Ageorges, N., & Walsh, J. R. 2002, ApJ, 573, L55

Jordan, C., Brueckner, G. E., Bartoe, J.-D. F., Sandlin, G. D., & van Hoosier, M. E. 1977, Nature, 270, 326

Kastner, J. H., Weintraub, D. A., Gatley, I., Merrill, K. M., & Probst, R. G. 1996, ApJ, 462, 777

Kruk, J. W., Durrance, S. T., Kriss, G. A., Davidsen, A. F., Blair, W. P., Espey, B. R., & Finley, D. S. 1995, ApJ, 454, L1

McCandliss, S. R. 2001, in ASP Conf. Ser. 247: Spectroscopic Challenges of Photoionized Plasmas, 523

McCandliss, S. R., France, K., Lupu, R. E., Burgh, E. B., Sembach, K., Kruk, J., Andersson, B.-G., & Feldman, P. D. 2006, ApJ, (in preparation)

Meaburn, J., Boumis, P., Christopoulou, P. E., Goudis, C. D., Bryce, M., & López, J. A. 2005, Revista Mexicana de Astronomia y Astrofisica, 41, 109

Meaburn, J., & Lopez, J. A. 1993, MNRAS, 263, 890

Meyer, D. M., Lauroesch, J. T., Sofia, U. J., Draine, B. T., & Bertoldi, F. 2001, ApJ, 553, L59

Monteiro, H., Morisset, C., Gruenwald, R., & Viegas, S. M. 2000, ApJ, 537, 853

Moos, H. W., et al. 2000, ApJ, 538, L1

O'Dell, C. R., Balick, B., Hajian, A. R., Henney, W. J., & Burkert, A. 2002, AJ, 123, 3329

Osterbrock, D. E., Fulbright, J. P., Martel, A. R., Keane, M. J., Trager, S. C., & Basri, G. 1996, PASP, 108, 277

Pottasch, S. R. 1996, A&A, 307, 561

Pottasch, S. R., Gilra, D. P., & Wesselius, P. R. 1982, A&A, 109, 182

Rachford, B. L., et al. 2002, ApJ, 577, 221

Rauch, T. 2003, A&A, 403, 709

Raymond, J. C., Blair, W. P., & Long, K. S. 1997, ApJ, 489, 314

Sahnow, D. J., et al. 2000, ApJ, 538, L7

Schwartz, R. D. 1983, ApJ, 268, L37

Shull, J. M. 1978, ApJ, 224, 841

Speck, A. K., Meixner, M., Jacoby, G. H., & Knezek, P. M. 2003, PASP, 115, 170

Spitzer, L. 1978, Physical processes in the interstellar medium (New York Wiley-Interscience, 1978. 333 p.)

Stecher, T. P., & Williams, D. A. 1967, ApJ, 149, L29

Sterling, N. C., Dinerstein, H. L., & Bowers, C. W. 2002, ApJ, 578, L55

Sternberg, A. 1989, ApJ, 347, 863

Storey, J. W. V. 1984, MNRAS, 206, 521

Takami, M., Usuda, T., Sugai, H., Kawabata, H., Suto, H., & Tanaka, M. 2000, ApJ, 529, 268

Torres-Peimbert, S., & Peimbert, M. 1977, Revista Mexicana de Astronomia y Astrofisica, 2, 181

Witt, A. N., Stecher, T. P., Boroson, T. A., & Bohlin, R. C. 1989, ApJ, 336, L21

Wolniewicz, L., Simbotin, I., & Dalgarno, A. 1998, ApJS, 115, 293

Wolven, B. C., Feldman, P. D., Strobel, D. F., & McGrath, M. A. 1997, ApJ, 475, 835

Wood, B. E., Karovska, M., & Raymond, J. C. 2002, ApJ, 575, 1057

Zuckerman, B., & Gatley, I. 1988, ApJ, 324, 501